# Nickel oxide thin films grown by dc reactive magnetron sputtering at various target to substrate distances

A. MALLIKARJUNA REDDY[a,b,*], SEUNG KI JOO[b], CHANG WOO BYUN[b], A. SIVASANKAR REDDY[c], P. SREEDHARA REDDY[a]

[a] *Department of Physics, Sri Venkateswara University, Tirupati 517502, India*

[b] *Research Institute of Advanced Materials, Department of Material Science and Engineering, Seoul National University, Seoul 151-744, Republic of Korea*

[c] *Division of Advanced Materials Engineering, Kongju National University, Cheonan City, Republic of Korea*

Nickel oxide (NiO) thin films were deposited on glass substrates at different target to substrate distances by dc reactive magnetron sputtering technique. It was observed that target to substrate distance has a great influence on the physical properties of the deposited films. The crystallite size of the films is reduced with increasing the target to substrate distance and the preferential orientation of the films was also changed. The optical results revealed that the optical transmittance of the films increased with increasing the target to substrate distance up to 70 mm thereafter it was decreased. The NiO films exhibit optical transmittance of 60 % and direct band gap of 3.82 eV at the target to substrate distance of 70 mm. The electrical resistivity decreases as target to substrate distance increases from 50 to 70 mm.

(Received May 16, 2012; accepted October 20, 2012)

*Keywords:* Reactive sputtering, Target to substrate distance, Structural properties, Optical properties

## 1. Introduction

Nickel oxide (NiO) is a Mott-Hubbard insulator [1, 2] that crystallizes in a rock salt structure (i.e NaCl-type structure). The lattice contracts along one of its body diagonals and undergoes a cubic to rhombohedral phase transformation below the Neel temperature [3]. NiO is a metal-deficient p-type semiconductor [4] and is a promising material for applications such as antiferromagnetic material [5], counter electrode in electrochromic smart windows [6], gas sensors [7], p-type transparent conducting electrodes [8], thermoelectric devices [9] and magnetoresistance sensors [10] etc. Thin films of p-type semiconductors are required in many optoelectronic device applications, which make use of hole injection. NiO is an interesting candidate of this class with a wide optical band gap of 3.6-4.0 eV [11]. NiO is considered to be a model semiconductor of hole-type conductivity. Nickel oxide is one of the uncommon p-type large band gap oxide material, It is an interesting material to study thin film properties, and possibility of manufacturing by variety of techniques such as sputtering [12], vacuum evaporation [13], electron beam evaporation [14], chemical vapour deposition [15], dip coating, spin coating, electro deposition [16] and spray pyrolysis [17]. It is evident that the improvement of the material properties can be reached by the optimization of the preparation conditions. Among these methods, reactive sputtering is one of the useful techniques having high deposition rates, uniformity over large areas of the substrates and easy control over the composition of the deposited films. In sputtering technique film properties were strongly depending on deposition parameters such as oxygen partial pressure, substrate temperature, sputtering power, sputtering pressure and target to substrate distance etc. Among these target to substrate distance is one of the most influenced parameter. In the present study, NiO thin films were deposited using dc reactive magnetron sputtering technique and the effect of target to substrate distance on the structural, morphological, optical and electrical properties was studied.

## 2. Experimental

NiO thin films were grown on Corning 7059 glass substrates using the dc reactive magnetron sputtering from a homemade circular planar magnetron sputtering system. The sputtering system is capable of creating an ultimate vacuum of $5 \times 10^{-4}$ Pa. The sputter chamber was pumped with diffusion pump and rotary pump combination. The pressure in the sputter chamber was measured using digital Pirani and Penning gauge combination. A circular planar magnetron of 100 mm diameter was used as the magnetron cathode. The magnetron target assembly was mounted on the top of the sputter chamber such that the sputtering could be done by sputter down configuration. A continuously variable dc power supply of 1000 V and 1 A was used as a power source for sputtering. A 100 mm diameter and 3 mm thick pure nickel (99.98%) was used as sputter target. Pure argon was used as sputter gas and oxygen as reactive gas. The flow rates of both argon and oxygen gases were controlled individually by Tylan mass flow controllers. Before deposition of each film, the target was sputtered in pure argon atmosphere for 10 min to remove oxide layer if any on the surface of the target. NiO thin films were deposited at various target to substrate distances in the range of 50 to 90 mm by keeping the other deposition conditions such as oxygen partial pressure, substrate temperature, sputtering power and sputtering pressure as constant. The crystallographic structure, surface morphology, optical and electrical properties were studied by various characterization techniques. A Scinco made instrument of model SMD 3000 was used for the measurement of film thickness. The crystallographic structure of the films was analyzed by X-ray diffractometer using Cu $K_\alpha$ radiation ($\lambda$ = 0.1546 nm) of model 3033TT manufactured by Seifert. The surface microstructure was studied by Carl Zeiss EVO MA 15 scanning electron microscopy (SEM). Atomic force microscopy (AFM) manufactured by Park Systems was used for surface morphology studies. The optical properties of the films were determined by Perkin Elmer Lambda 950 UV-Vis-NIR double beam spectrophotometer. The optical absorption coefficient ($\alpha$) was calculated from the optical transmittance (T) and reflectance (R) data using the relation

$$\alpha = -1/t \, [\ln T/(1-R)^2 ] \qquad (1)$$

where t is the thickness of the film.

The dependence of $\alpha$ on the photon energy ($h\nu$) fitted to the relation for direct transition

$$\alpha h\nu = A\,(h\nu - E_g)^{1/2} \qquad (2)$$

where $E_g$ is the optical band gap of the films.

The electrical resistivity and Hall mobility were carried out by employing the Van der Pauw method. The sputtering conditions maintained during the growth of NiO films were given in Table 1.

*Table 1. Deposition parameters maintained during the deposition of NiO films by dc reactive magnetron sputtering.*

| | |
|---|---|
| Sputtering target pure nickel (99.98%) | 100 mm diameter and 3 mm thick |
| Target to substrate distance | 50-90 mm |
| Substrates | Corning 7059 glass |
| Ultimate pressure ($P_U$) | 5 × $10^{-4}$ Pa |
| Oxygen partial pressure ($pO_2$) | 6 × $10^{-2}$ Pa |
| Sputtering pressure ($P_W$) | 4 Pa |
| Substrate temperature ($T_S$) | 523 K |
| Sputtering power | 150 W |
| Sputtering time | 6-14 Minutes |

## 3. Results and discussion

### 3.1. Structural properties

The thickness of the deposited films was constantly maintained as 350 nm at different target to substrate distances by varying the deposition time. The XRD profiles of NiO thin films as a function of the target to substrate distance was shown in Fig. 1 and from the XRD results, it was observed that all the deposited films were polycrystalline and retain rock salt structure. The films exhibited (111) and (200) orientations and the intensity of these orientations decreased with increase of target to substrate distance from 50 to 60 mm. This may be due to the kinetic energy of sputtered particles/atoms when arriving at the substrate. Smaller target to substrate distances would enable the particles/atoms to reach the substrate with higher energy, leading to an increase in the substrate temperature. This means that more opportunity is provided for atoms to move around on the substrate and form larger crystallites in the films [18]. Thereafter at target to substrate distance of 70 mm, the orientation was shifted to (220) with crystallite size of 29.17 nm. On further increasing the target to substrate distance to 80 mm, the intensity of the peak was reduced. Orientation of the films was again changed to (111) and (200) at higher target to substrate distance of 90 mm. The nucleations with various orientations can be formed at the initial stage of the deposition and each nucleus competes to grow but only nuclei having the fastest growth can survive.

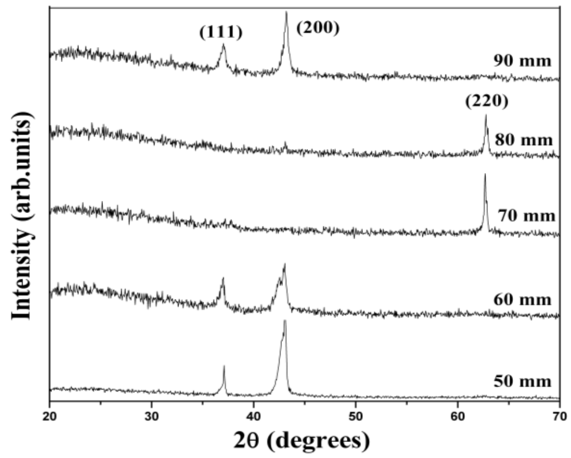


*Fig. 1. X-ray diffraction patterns of NiO films deposited at various target to substrate distances.*

However, in literature the decrease in crystallinity without any orientation change as function of target to substrate distance was reported in rf sputtered films [19,20]. The orientation of the films is thought to be dependent on the mobility of adatoms and clusters on the substrate [21]. The lattice parameter of the films was also influenced by the target to substrate distance. The present obtained lattice parameter of as deposited films is higher than the standard bulk NiO. The variation in the lattice parameter with target to substrate distance was due to the stress developed in the films. The stress (σ) developed in the films was calculated from the X-ray diffraction data employing the relation [22]

$$\sigma = -E(a-a_o)/2\nu a_o$$

where E is the Young's modulus of the NiO (200 GPa), a is the lattice parameter of the bulk material, $a_o$ is the measured lattice parameter and ν is the Poisson's ratio (0.31). The tensile stress developed in the films is due to the existence of microscopic voids incorporated in the films during condensation [23]. The lattice parameter, crystallite size and stress of the NiO films as a function of target to substrate distance were given in Table 2.

*Table 2. Structural information of dc reactive magnetron sputtered NiO films at various target to substrate distances.*

| T-S distance (mm) | Orientation | Lattice Parameter (nm) | Crystallite size (nm) | Stress (GPa) |
|---|---|---|---|---|
| 50 | (111) | 0.4193 | 40.52 | 1.3670 |
| | (200) | 0.4198 | 13.07 | 1.6920 |
| 60 | (111) | 0.4205 | 22.96 | 2.2760 |
| | (200) | 0.4204 | 08.61 | 2.1690 |
| 70 | (220) | 0.4189 | 29.17 | 1.0009 |
| 80 | (220) | 0.4184 | 22.64 | 0.6167 |
| 90 | (111) | 0.4202 | 11.87 | 1.9960 |
| | (200) | 0.4184 | 19.11 | 0.6168 |

### 3.2. Surface morphology

The scanning electron microscopy images of NiO films formed at different target to substrate distances were shown in Fig. 2. It was observed that the films having smooth surface at target to substrate distance of 50 mm, and the small grains were appeared at target to substrate distance of 60 mm. Thereafter at target to substrate distance of 70 mm fine grains were appeared. At 80 mm target to substrate distance the grain growth was non uniform. The grain growth was reduced at 90 mm target to substrate distance.

The AFM micrographs of NiO films deposited at various target to substrate distances were shown in Fig. 3. The AFM micrograph of NiO film deposited at target to substrate distance of 50 mm, the films showed surface roughness of 7.9 nm. As the target to substrate distance increased to 70 mm, uniform grains were observed with

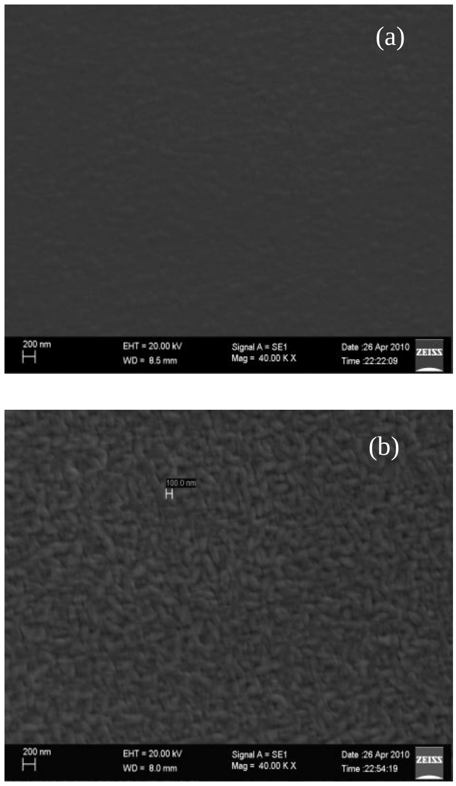


*Fig. 2. SEM images of NiO films at target to substrate distance of (a) 60 mm (b) 80 mm.*

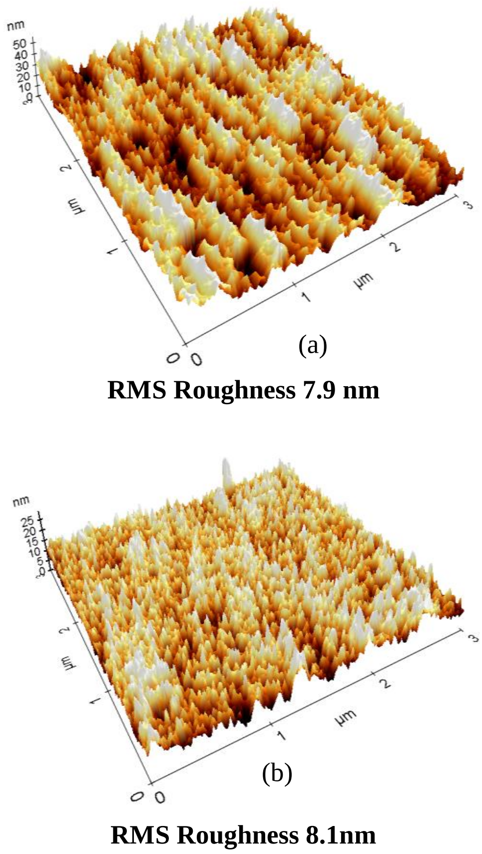


*Fig. 3. AFM images of NiO films deposited at target to substrate distances of (a) 50 mm (b) 90 mm.*

increased surface roughness of 9.4 nm. The decreasing of grain size and the surface roughness was observed at higher target to substrate distances.

### 3.3. Optical and electrical properties

Fig. 4 shows the optical transmittance spectra of NiO films as a function of target to substrate distance. The optical transmittance of the films increased from 18 to 60 % with increasing of target to substrate distance from 50 to 70 mm. On further increasing the target to substrate distance to 90 mm, the transmittance of the films decreased to 28 %. The absorption edge was shifted towards lower wavelength with the increase of target to substrate distance upto 70 mm. The increase in transmittance of the films is related to an increase in grain size of the films.

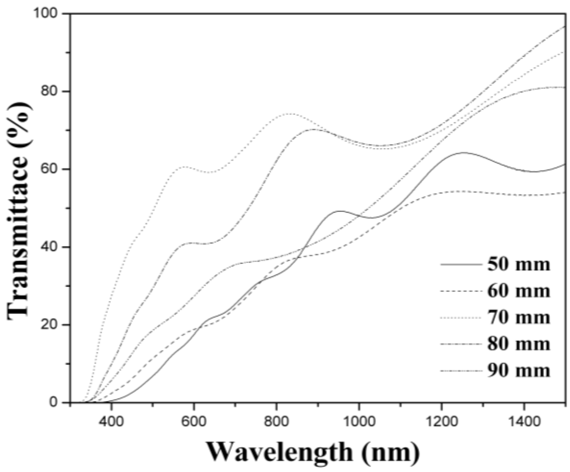


*Fig. 4. Optical transmittance spectra of NiO films as a function of target to substrate distance.*

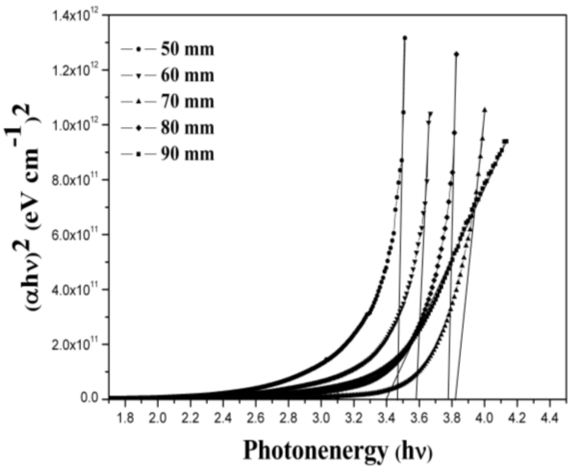


*Fig. 5. Plot of $(\alpha h\nu)^2$ and $(h\nu)$ for the NiO films deposited at various target to substrate distances.*

The plots of $(\alpha h\nu)^2$ versus photon energy ($h\nu$) of the NiO films formed at various target to substrate distances were shown in Fig. 5. The optical band gap of the films was evaluated from the extrapolation of the linear portion of the plots of $(\alpha h\nu)^2$ versus ($h\nu$) to $\alpha = 0$. The optical band gap of the films increased from 3.46 to 3.82 eV with the increase of target to substrate distance from 50 to 70 mm, beyond this target to substrate distance the optical band gap of NiO films was decreased to 3.40 eV. The values of optical transmittance and band gap of each target to substrate distance were summarized in Table 3. Reported optical band gap for NiO films are in the range of 3.15-3.80 eV [24], our results are in good agreement with the reported results in the literature.

The electrical resistivity of undoped NiO has a strong dependence on the microstructural defects existing in NiO crystallites, such as nickel vacancies and interstitial defects [25]. It is clear that electrical properties of NiO thin films are greatly affected by target to substrate distance. The films showed high electrical resistivity of 37.29 Ωcm at target to substrate distance of 60 mm and low electrical resistivity of 5.1 Ωcm at target to substrate distance of 70 mm. The electrical conductivity of the NiO films was more favorable to (220) orientation as compare to (200) and it was also observed from XRD results. The improvement of grain size, decrease in the grain boundary, which minimized the trapping and/or scattering of charge carriers at the grain boundaries. The electrical and optical results conclude that the (220) orientation was most favorable to the improvement of the electrical conductivity and optical transmittance caused by the improvement of the grain size and hence minimized the scattering of charge carriers at grain boundaries and surface light scattering respectively.

*Table 3. Optical and electrical information of dc reactive magnetron sputtered NiO films at various target to substrate distances.*

| T-S distance (mm) | Transmittance (%) | Optical band gap (eV) | Resistivity (Ωcm) |
|---|---|---|---|
| 50 | 18 | 3.46 | 19.05 |
| 60 | 19 | 3.59 | 37.29 |
| 70 | 60 | 3.82 | 05.10 |
| 80 | 41 | 3.78 | 16.83 |
| 90 | 28 | 3.40 | 30.18 |

## 4. Conclusions

The polycrystalline nickel oxide (NiO) thin films were successfully deposited by dc reactive magnetron sputtering at different target to substrate distances. The films deposited at target to substrate distance of 70 mm exhibited (220) as preferred orientation with grain size of 29.17 nm. The films showed high electrical resistivity of 37.29 Ωcm at target to substrate distance of 60 mm.

## References

[1] B. H. Brandow, Adv. Phy. **26,** 651 (1997).
[2] M. R. Norman, Phy. Rev. Lett. **64,** 1162 (1990).
[3] G. A. Slack, J. Appl. Phys. **31,** 1571 (1960).
[4] E. Fujji, A. Tomozawa, H. Torii, R. Takayama, Jpn. J. Appl. Phys. **35**, L328 (1996).
[5] H. Sato, T. Minami, S. Takata, T. Yamada, Thin Solid Films **236**, 27 (1993).
[6] C. M. Lampert, C. G. Granqvist, large-area chromogenics: materials and devices for transmittance control (SPIE Opt. Engr. Press, Bellingham, USA, 1990).
[7] I. Hotovy, J. Huran, P. Siciliano, S. Capone, L. Spiess, V. Rehacek, Sensors Actuators B **78**, 126 (2001).
[8] I.-M. Chan, T.-Y. Hsu, F. C. Hong, Appl. Phys. Lett. **81**, 1899 (2002).
[9] W. Shin, N. Murayama, Mater. Lett. **45**, 302 (2000).
[10] M. J. Carey, A. E. Berkowitz, J. Appl. Phys. **73,** 6892 (1993).
[11] D. Adler, J. Feinleib, Phy. Rev. B **2**, 3112 (1970).
[12] K. Yoshimura, T. Miki, S. Tanemura, Jpn. J. Appl. Phys. **34**, 2440 (1995).
[13] B. Sasi, K. G. Gopchandran, P. K. Manoj, P. Koshy, P. Prabhakara Rao, V. K. Vaidyan, Vacuum **68**, 149 (2002).
[14] T. Seike, J. Nagai, Solar Energy Mater. **22**, 107 (1991).
[15] T. Maruyama, S. Arai, Sol. Energy Mater. Sol. Cells **30**, 257 (1993).
[16] F. Vera, R. Schrebler, E. Munoz, C. Suarez, P. Cury, A. Gomez. R. Cordova, R. E. Marotti, E. A. Dalchiele, Thin Solid Films **490,** 182 (2005).
[17] D. Desai, S. K. Min, K.-D. Jung, O.-S. Joo, Appl. Surf. Sci. **253**, 1781 (2006).
[18] L. Chen, X. Bi, Vacuum **82**, 1216 (2008).
[19] G. Natarajan, S. Daniels, D. C. Cameron, P. J. McNally, Thin Solid Films **516**, 5531 (2008).
[20] S. H. Jeong, J. H. Boo, Thin Solid Films **447-448,** 105 (2004).
[21] Y. S Jung, S. S Lee, J. Cryst. Growth **259,** 343 (2003).
[22] M. Ohring, The material science of Thin Solid Films (Academic Press, New York, 1992).
[23] W. Buckel, J. Vac. Sci. Technol. **6**, 606 (1969).
[24] P. Puspharajah, S. Radhakrishna, A. K. Arof, J. Mater. Sci. **32**, 3001 (1997).
[25] E. Antolini, J. Mater. Sci. **27**, 3335 (1992).

*Corresponding author: amreddy81@gmail.com